



## Strategy of EMIC Wave Observation by Arase/PWE and its Initial Results

S. Matsuda<sup>(1)</sup>, Y. Kasahara<sup>(2)</sup>, Y. Miyoshi<sup>(1)</sup>, R. Nomura<sup>(3)</sup>, S. Kurita<sup>(1)</sup>, M. Teramoto<sup>(1)</sup>, Y. Kasaba<sup>(4)</sup>, K. Ishisaka<sup>(5)</sup>, M. Shoji<sup>(1)</sup>, and A. Matsuoka<sup>(6)</sup>

(1) Institute for Space-Earth Environmental Laboratory, Nagoya University, Nagoya, JAPAN

(2) Graduate School of Natural Science and Technology, Kanazawa University, Kanazawa, JAPAN

(3) Japan Aerospace Exploration Agency (JAXA), Tsukuba, JAPAN

(4) Graduate School of Science, Tohoku University, Sendai, JAPAN

(5) Department of Information Systems Engineering, Toyama Prefectural University, Imizu, JAPAN

(6) Institute of Space and Astronautical Science, Sagami-hara, JAPAN

### Abstract

We developed the onboard processing software for the Plasma Wave Experiment (PWE) onboard Arase, and established strategies of EMIC wave observation. We measure 64/256 Hz sampling electric field waveform by Electric Field Detector (EFD), and 1024 Hz sampling electric/magnetic field waveforms by Waveform Capture (WFC). We successfully obtained EMIC waves along the orbit by using these observation modes depending on the region. 166 EMIC waves were observed during 9 months (from March to November 2017), and approximately 37% of observed EMIC waves showed fine rising-tone structures (similar to that of Pc1 pearl pulsations observed by ground magnetometer observations). We performed statistical analyses of observed EMIC waves, and found that the occurrence probability of unstructured EMIC waves is clearly high around dusk-side, while that of fine-structured EMIC waves (Pc1 pearl pulsations) is high around noon. This suggests that the generation and/or propagation mechanism of these two types EMIC waves are different.

### 1 Introduction

The wave-particle interaction process has an important role for the electron acceleration and loss in the terrestrial inner magnetosphere. Particularly, the significant loss of relativistic electron and energetic ion precipitation due to electromagnetic ion cyclotron (EMIC) waves is a remarkable process [1, 2, 3, 4, 5]. Statistical analyses of EMIC waves around radiation belts have been performed by using data obtained by the Van Allen probes, and they clarified local time dependence of EMIC waves in the inner magnetosphere [6, 7]. The Arase satellite was launched on December 20, 2016 to understand dynamics around the Van Allen radiation belt such as particle acceleration, loss mechanisms, and the dynamic evolution of space storms in the context of cross-energy and cross-regional coupling [8, 9]. The Plasma Wave Experiment (PWE) is one of the scientific instruments onboard the Arase satellite and measures the electric field and magnetic field in the inner magnetosphere

[10]. A great advantage of Arase's observation is its latitudinal coverage. Because the orbital inclination of Arase is 31 degrees, the satellite has many chances to observe not only around the geomagnetic equatorial region but around mid-latitude region. In this paper, we introduce our strategy of EMIC waves observation by PWE onboard Arase, and its initial results.

### 2 Specification of Arase/PWE for EMIC Waves Observation

The PWE covers frequency range from DC to 10 MHz for electric field, and from a few Hz to 100 kHz for magnetic field by the following receivers: Electric Field Detector (EFD) [11] for the measurement of electric field from DC to 256 Hz, Waveform Capture/Onboard Frequency Analyzer (WFC/OFA) [12] for the measurement of electric field and magnetic field from a few Hz to 20 kHz, and the High Frequency Analyzer (HFA) [13] for the measurement of electric field from 10 kHz to 10 MHz and magnetic field from 10 to 100 kHz. For EMIC wave observation, low-rate (64/256 Hz) electric field waveform obtained by EFD and mid-rate electric and magnetic field waveforms obtained by WFC/OFA are important. Low-rate (64/256 Hz) magnetic field waveform is observed by the Magnetic Field Experiment (MGF) [17]. We can analyze EMIC waves by combining the electric and magnetic field waveforms obtained by EFD and MGF.

The WFC measures waveforms of two-electric and three-magnetic field components. The typical frequency range of EMIC waves are below the local proton cyclotron frequency ( $f_{cH^+}$ ) and corresponds to a range from a few Hz to several hundred Hz in the inner magnetosphere [14, 15, 16]. Since the original sampling-rate of WFC (65536 Hz) is too high to observed EMIC waves, we installed a special operation mode for EMIC waves observation. The "EMIC burst mode" measures electric and magnetic field waveform data at a low sampling rate (1024 samples/s). Since the proton cyclotron frequency along the orbit of Arase is typically below 300 Hz, EMIC burst mode is sufficient for the magnetosonic wave measurement. The amount of data is 1/64

of original waveform, hence we can obtain waveforms for long periods. This is enabled by the down-sampling technique realized by a combination of decimation filters. We perform 1/64 decimation of observed waveforms by using the cascaded decimation filter as shown in Figure 1.

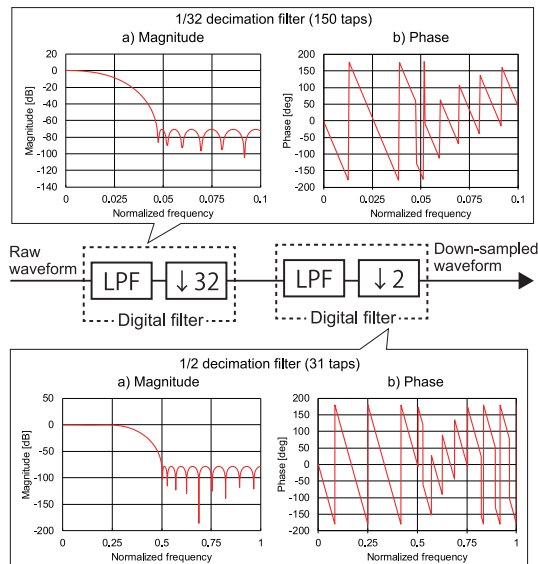


**Figure 1.** A block diagram of the cascaded decimation filter.

### 3 Observation Strategy

Figure 2 shows the strategy of EMIC wave observation by PWE. Since the proton cyclotron frequency ( $f_{H^+}$ ) along the orbit of Arase varies from few Hz to few hundred Hz, we organize nominal operation plan for the EMIC wave observation as follows [10]:

- When the Arase satellite is located outside of the plasmapause ( $L > 4$ ), we change the sampling frequency of EFD to 64 Hz in cooperation with the MGF to focus on EMIC waves less than 30 Hz.
- When the Arase satellite is located in the plasmasphere ( $L < 4$ ) where ion cyclotron frequency exceeds 30 Hz, we change the sampling frequency of EFD to 256 Hz to cover ion mode waves. The MGF will also measure magnetic waveforms sampled at 256 Hz.

We obtain 3 minutes' continuous waveforms of two-electric and three-magnetic field components every 12 minutes by WFC/EMIC burst mode. We operate the EMIC burst mode in the entire region along the orbit except when we operate the other burst mode (each mode is exclusively operated).

### 4 EMIC waves observed by Arase/PWE

We surveyed waveform data obtained by PWE onboard Arase for 9 months (from March to November 2017), and found that 166 EMIC waves were observed during the

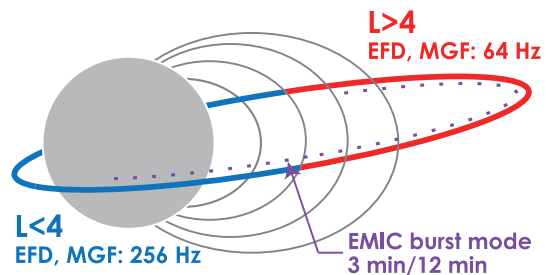


**Figure 2.** The overview of the strategy of EMIC wave observation by Arase/PWE.

period. Figure 3 is electric field dynamic power spectrum observed on 8 September 2017. Gray solid lines in the figure indicate local proton ( $f_{H^+}$ ), helium ( $f_{He^+}$ ), and oxygen ( $f_{O^+}$ ) ion cyclotron frequency calculated from the DC magnetic field measurement by MGF. EMIC waves were observed during the period from 2 to 10 Hz. A clear gap around helium ion cyclotron frequency ( $f_{He^+}$ ) can be explained by the linear theory of ion cyclotron mode waves.

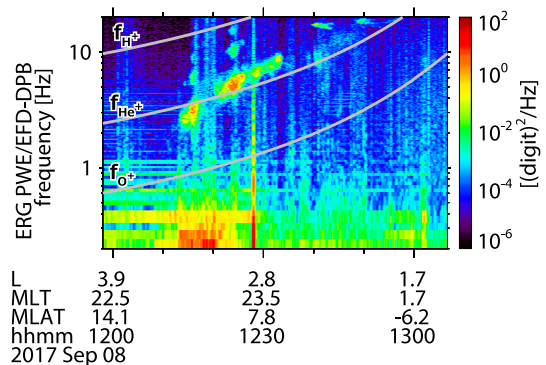
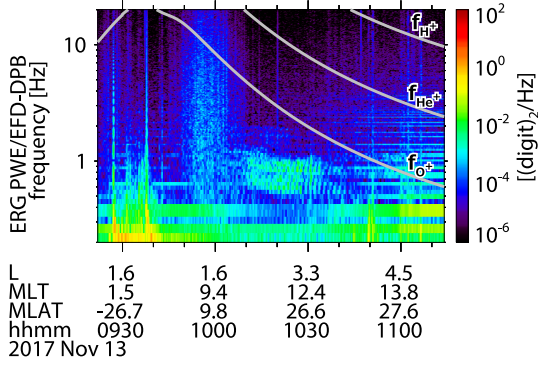


**Figure 3.** Electric field dynamic power spectrum of unstructured EMIC waves observed by Arase/PWE on 8 September 2017.

Figure 4 shows the electric field dynamic power spectrum of the other example of EMIC waves observed by PWE onboard Arase on 13 November 2017. The EMIC wave was observed during the period from 0.5 to 1 Hz (below the oxygen ion cyclotron frequency). The EMIC wave had a fine rising-tone structure (similar to that of Pc1 pearl pulsations observed by ground radio observations). Approximately 37% of observed EMIC waves obtained by the PWE has such fine structures.

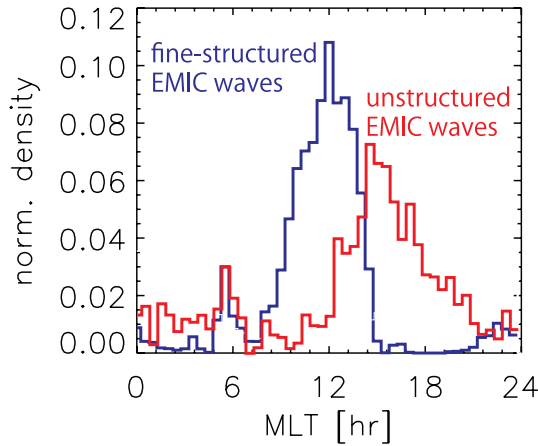
### 5 Statistical Analyses

Figure 5 shows magnetic local time dependence of unstructured EMIC waves (red line) and fine-structured EMIC waves (blue line) observed by Arase/PWE during the period. Occurrence probability is normalized to spacecraft dwell time. We found that the occurrence probability of unstructured EMIC waves is clearly high around dusk-side. This is consistent with the previous satellite observation (e.g. AMPTE/CCE observation [18]) and well-recognized



**Figure 4.** Electric field dynamic power spectrum of fine-structured EMIC waves observed by Arase/PWE on 13 November 2017.

theory of drift path of fresh ring current ions. On the other hand, occurrence probability of fine-structured EMIC waves (Pc1 pearl pulsations) is high around noon region. This suggests that the generation and/or propagation mechanism of these two types EMIC waves are different.



**Figure 5.** Magnetic local time dependence of unstructured EMIC waves (red line) and fine-structured EMIC waves (blue line) observed by Arase/PWE. Occurrence probability is normalized to spacecraft dwell time.

Figure 6 shows spatial distributions of fine-structured EMIC waves (left) and that of unstructured EMIC waves (right) observed by Arase/PWE. Occurrence probabilities were normalized to spacecraft dwell time. We found that the spatial distribution of the fine-structured EMIC waves is greatly different from that of the unstructured EMIC waves.

1. Fine-structured EMIC waves (Pc1 pearl pulsations) were observed around a specified L-shell (approximately  $L=3-4$ ). This suggests that the fine-structured EMIC waves propagate along the geomagnetic field line near the plasmapause.
2. Occurrence probability of the fine-structured EMIC waves was relatively low around geomagnetic equatorial region compare to that of the unstructured EMIC

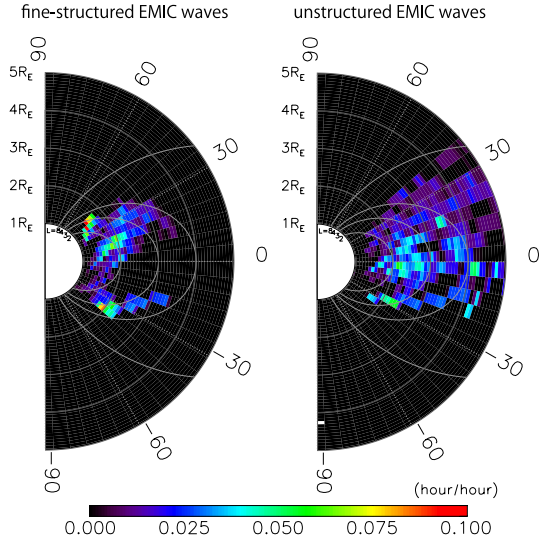


**Figure 6.** Spatial distributions of fine-structured EMIC waves (left) and that of unstructured EMIC waves (right) observed by Arase/PWE. Occurrence probabilities are normalized to spacecraft dwell time.

waves. This trend is consistent with the Van Allen probes observation reported by *Paulson et al. (2017)*.

3. The spatial distribution of the fine-structured EMIC waves showed a clear latitudinal dependence. Occurrence probability was relatively high around the low-altitude or high-latitude region. This suggests that the formation of such fine-structures of EMIC waves is related to the effect of wave propagation.

## 6 Summary

We presented onboard signal processing techniques and observation strategies of Arase/PWE for the EMIC waves observation. We successfully obtained 166 EMIC waves during first 9 months after the satellite was launched. Our statistical analyses showed that the spatial distributions of the unstructured EMIC waves and that of the fine-structured EMIC waves were greatly different. Occurrence probability of the fine-structured EMIC waves had a clear peak around noon. We also showed the spatial distribution of the fine-structured EMIC waves, and found that they were observed around a specified L-shell (approximately  $L=3-4$ ). The wide latitudinal coverage of Arase's orbit enabled this unique analysis. Further studies (e.g. investigation of Kp dependence) are necessary to clarify the variation of EMIC waves distribution.

## 7 Acknowledgements

This research was supported by a Grant-in-Aid for Scientific Research from the Japan Society for the Promotion of Science (#14J02108, #15H05815, #15H05747, #16J02163, and #17K05668), and Grant-in-Aid for JSPS Fellows.

## References

- [1] Cornwall, J. M. (1965), Cyclotron instabilities and electromagnetic emission in the ultra low frequency and very low frequency ranges, *J. Geophys. Res.*, *70(1)*, 61–69, doi:10.1029/JZ070i001p00061.
- [2] Albert, J. M. (2003), Evaluation of quasi-linear diffusion coefficients for EMIC waves in a multi-species plasma, *J. Geophys. Res.*, *108(A6)*, 1249, doi:10.1029/2002JA009792.
- [3] Horne, R., and R. M. Thorne (1998), Potential waves for relativistic electron scattering and stochastic acceleration during magnetic storms, *Geophys. Res. Lett.*, *25*, 3011–3014.
- [4] Meredith, N. P., R. M. Thorne, R. B. Horne, D. Summers, B. J. Fraser, and R. R. Anderson (2003), Statistical analysis of relativistic electron energies for cyclotron resonance with EMIC waves observed on CRRES, *J. Geophys. Res.*, *108(A6)*, 1250, doi:10.1029/2002JA009700.
- [5] Thorne, R. M., and C. F. Kennel (1971), Relativistic electron precipitation during magnetic storm main phase, *J. Geophys. Res.*, *76(19)*, 4446–4453, doi:10.1029/JA076i019p04446.
- [6] Wang, D., Z. Yuan, X. Yu, X. Deng, M. Zhou, S. Huang, H. Li, Z. Wang, Z. Qiao, C. A. Kletzing, and J. R. Wygant (2015), Statistical characteristics of EMIC waves: Van Allen Probe observations. *J. Geophys. Res. Space Physics*, *120*, 4400–4408. doi:10.1002/2015JA021089.
- [7] Paulson, K. W., C. W. Smith, M. R. Lessard, R. B. Torbert, C. A. Kletzing, and J. R. Wygant (2017), In situ statistical observations of Pc1 pearl pulsations and unstructured EMIC waves by the Van Allen Probes, *J. Geophys. Res. Space Physics*, *122*, 105–119, doi:10.1002/2016JA023160.
- [8] Miyoshi, Y. et al. (2012), The Energization and Radiation in Geospace (ERG) Project, in *Dynamics of the Earth's Radiation Belts and Inner Magnetosphere* (eds D. Summers, I. R. Mann, D. N. Baker and M. Schulz), 103–116, doi: 10.1029/2012GM001304
- [9] Miyoshi, Y., I. Shinohara, T. Takashima, K. Asamura, N. Higashio, T. Mitani, S. Kasahara, S. Yokota, Y. Kazama, S.-Y. Wang, P. Ho, Y. Kasahara, Y. Kasaba S. Yagitani, A. Matsuoka, H. Kojima, Y. Katoh, K. Shiokawa, K. Seki (2017), Geospace Exploration Project ERG; overview, *Earth, Planets and Space*.
- [10] Kasahara, Y., Y. Kasaba, H. Kojima, S. Yagitani, K. Ishisaka, A. Kumamoto, F. Tsuchiya, M. Ozaki, S. Matsuda, T. Imachi, Y. Miyoshi, M. Hikishima, Y. Katoh, M. Ota, M. Shoji, A. Matsuoka, and I. Shinohara (2017), The Plasma Wave Experiment (PWE) on board the Arase (ERG) Satellite, *Earth, Planets and Space*, doi:10.1186/s40623-017-0759-3.
- [11] Kasaba, Y., K. Ishisaka, Y. Kasahara, T. Imachi, S. Yagitani, H. Kojima, S. Matsuda, M. Shoji, S. Kurita, T. Hori, A. Shinbori, M. Teramoto, Y. Miyoshi, T. Nakagawa, N. Takahashi, Y. Nishimura, A. Matsuoka, A. Kumamoto, F. Tsuchiya, and R. Nomura (2017), Wire Probe Antenna (WPT) and Electric Field Detector (EFD) of Plasma Wave Experiment (PWE) aboard Arase: Specifications and initial evaluation results, *Earth, Planets and Space*, doi:10.1186/s40623-017-0760-x.
- [12] Matsuda, S., Y. Kasahara, H. Kojima, Y. Kasaba, S. Yagitani, M. Ozaki, T. Imachi, K. Ishisaka, A. Kumamoto, F. Tsuchiya, M. Ota, S. Kurita, Y. Miyoshi, M. Hikishima, A. Matsuoka, and I. Shinohara (2018), Onboard Software of Plasma Wave Experiment aboard Arase: Instrument Management and Signal Processing of Waveform Capture/Onboard Frequency Analyzer, *Earth, Planets and Space*, doi:10.1186/s40623-017-0758-4.
- [13] Kumamoto, A., F. Tsuchiya, Y. Kasahara, Y. Kasaba, H. Kojima, S. Yagitani, K. Ishisaka, T. Imachi, M. Ozaki, S. Matsuda, M. Shoji, A. Matsuoka, Y. Katoh, Y. Miyoshi, and T. Obara (2017), High Frequency Analyzer (HFA) of Plasma Wave Experiment (PWE) onboard the Arase spacecraft, *Earth, Planets and Space*.
- [14] Mauk, B. H. (1982), Helium resonance and dispersion effects on geostationary Alfvén/ion cyclotron waves, *J. Geophys. Res.*, *87(A11)*, 9107–9119, doi:10.1029/JA087iA11p09107.
- [15] Gomberoff, L. and R. Neira (1983), Convective growth rate of ion-cyclotron waves in a  $H^+ - He^+$  and  $H^+ - He^+ - O^+$  plasma, *J. Geophys. Res.*, *88* 2170.
- [16] Gendrin, R., M. Ashour-Abdalla, Y. Omura, and K. Quest (1984), Linear analysis of ion cyclotron interaction in a multicomponent plasma, *J. Geophys. Res.*, *89(A10)*, 9119–9124, doi:10.1029/JA089iA10p09119.
- [17] Matsuoka, A., M. Teramoto, R. Nomura, M. Nosé, A. Fujimoto, Y. Tanaka, M. Shinohara, T. Nagatsuma, K. Shiokawa, Y. Obana, Y. Miyoshi, M. Mita, T. Takashima, and I. Shinohara (2017), The Arase(ERG) magnetic field investigation, *Earth, Planets and Space*.
- [18] Anderson, B. J., R. E. Erlandson, and L. J. Zanetti (1992), A statistical study of Pc1-2 magnetic pulsations in the equatorial magnetosphere: 1. Equatorial occurrence distributions, *J. Geophys. Res.*, *97*, 3075–3088, doi:10.1029/91JA02706.